RSC Advances

RSC Publishing

COMMUNICATION

View Article Online
View Journal | View Issue

Published on 12 March 2013. Downloaded by University of Western Ontario on 30/10/2014 19:55:39.

Direct conversion of calcium carbonate to C_1–C_3 hydrocarbons†

Cite this: *RSC Advances*, 2013, **3**, 7224

Received 17th January 2013,
Accepted 11th March 2013

DOI: 10.1039/c3ra40264a

www.rsc.org/advances

D. Jagadeesan,[a] Y. Sundarayya,[a] Giridhar Madras[b] and C. N. R. Rao*[a]

With the objective of investigating the direct conversion of inorganic carbonates such as $CaCO_3$ to hydrocarbons, assisted by transition metal ions, we have carried out studies on $CaCO_3$ in an intimate admixture with iron oxides (FeCaCO) with a wide range of Fe/Ca mole ratios (*x*), prepared by co-precipitation. The hydrogen reduction of FeCaCO at 673 K gives up to 23% yield of the hydrocarbons CH_4, C_2H_4, C_2H_6 and C_3H_8, leaving solid iron residues in the form of iron metal, oxides and carbide particles. The yield of hydrocarbons increases with *x* and the conversion of hydrocarbons occurs through the formation of CO. While the total yield of hydrocarbons obtained by us is comparable to that in the Fischer–Tropsch synthesis, the selectivity for C_2–C_3 hydrocarbons reported here is noteworthy.

Introduction

An important present-day global priority is to identify renewable sources of energy that can meet the demands of economic growth. It is important to remember that a serious emphasis is placed on the environmental sustainability of any new process associated with energy production. The combustion of fossil fuels, a major source of energy in the present-day economy, releases a staggering amount of CO_2 into the atmosphere[1] leading to adverse effects on climate and the environment. A promising approach to addressing the problems of energy availability, as well as environmental pollution, is to recycle CO_2 to produce commercially important chemicals.[1–4] This approach is realistic and would help in mitigating the increase in atmospheric CO_2 levels, and reduce our dependence on oil by producing carbon-neutral fuels and feedstock chemicals.[5,6] Since many of the materials for CO_2 sequestration may not be of practical use, it is important that the chemical utilization of CO_2 receives wider attention.[7–13] If an efficient CO_2 capture process and its subsequent chemical transformation is developed, the cost of energy production can be significantly lowered. CO_2 is sequestered in nature as solid carbonate minerals, and these mineral rocks are abundant. Inorganic carbonate minerals and the large volumes of industrial CO_2 which are being pumped into ocean beds as carbonates may too be utilized profitably by converting them into hydrocarbons.[14] Inorganic mineral carbonates have the potential to become a renewable resource for the production of fuels and chemicals as they can be rapidly replenished by the carbonation process. Fossil fuels such as coal and petrol are non-renewable for human use because of the long lag time of their natural formation. On the contrary, the rapid sequestration of CO_2 to inorganic carbonates will allow us to replenish it as a carbon resource quickly enough to meet global energy demands, thereby leading to a steady state-like condition. The process of accelerating the reaction of CO_2 with alkaline oxides and silicates to form carbonates is moving towards commercialization.[15] The use of H_2 during the catalytic reduction of $CaCO_3$ to hydrocarbons is inevitable and can be considered a non-green process. One hopes that it is not too optimistic to assume the production of H_2 will become an environmentally benign commercial reality in the future, for instance, through the photocatalytic splitting of H_2O. In this report, we discuss the hydrogenation of $CaCO_3$ to form C_1–C_3 hydrocarbons, in the presence of iron catalysts, a process which has the great potential to be developed further.

As part of our studies to convert inorganic carbonates to hydrocarbons, we have demonstrated that $CaCO_3$ containing transition metal ions such as Fe, Co and Ni can be transformed to CH_4 in the presence of H_2.[16] Under the experimental conditions employed in this work,[16] CH_4 was the only major product and the best catalyst contained Co, CoO and CaO. The earlier study employed a reaction pressure of 2–5 atm and a hydrogen-rich atmosphere which drove the reaction to form CH_4 exclusively. Interestingly, among the transition metal ions tested, iron appeared to show the formation of hydrocarbons (HCs) beyond CH_4. The catalytic role of iron-based catalysts in the production of long chain HCs is known in the Fischer–Tropsch (FT) synthesis

[a]*International Centre for Materials Science and CSIR Centre of Excellence in Chemistry, Jawaharlal Nehru Centre for Advanced Scientific Research, Jakkur P.O., Bangalore-560064, India. E-mail: cnrrao@jncasr.ac.in; Fax: 91 80 2365 3075; Tel: 91 80 2208 2760*

[b]*Department of Chemical Engineering, Indian Institute of Science, Bangalore-560012, India*

† Electronic supplementary information (ESI) available: XRD, Mössbauer, XPS, time on stream. See DOI: 10.1039/c3ra40264a

This journal is © The Royal Society of Chemistry 2013

Published on 12 March 2013. Downloaded by University of Western Ontario on 30/10/2014 19:55:39.

which utilizes CO + H_2 as the feed.[17,18] There is a renewed interest in Fe-based catalysts in the FT reaction due to their abundance, low-cost and unique ability to form oxygenates.[19] Unlike cobalt, the chemistry of iron catalysis involves the formation of oxide and carbide phases in addition to the formation of metallic iron. The exact role of each phase in the catalytic activity is a subject of scientific debate.[20] The motivation of the present work was to explore the selective conversion of solid inorganic carbonates to higher HC products using iron/iron oxides as catalysts. To our knowledge, such studies have not been reported in the literature.

Experimental section

Synthesis of carbonates

Calcium carbonate compositions were prepared according to the procedure reported earlier.[21] In a typical synthesis, 4.2 g $NaHCO_3$ was dissolved in 30 mL H_2O and maintained at 353 K. The solution was continuously bubbled with CO_2 from a pressurized container at a rate of 50 mL min^{-1} throughout the experiment. An aqueous solution of 20 mL containing 0.59 g $Ca(NO_3)_2 \cdot 4H_2O$ and a suitable quantity of $FeCl_2$ was added according to the required Fe/Ca mole ratio (x). The Fe salt solution was added dropwise to the $NaHCO_3$ solution under stirring. Precipitation was observed immediately. The mixture was stirred at 353 K for 30 min, after which it was allowed to cool to room temperature naturally. The precipitate was filtered, washed in water and dried at 333 K for 2 days. The dried samples did not contain chloride ions, as found by energy dispersive X-ray analysis.

Characterization

The starting carbonate materials contained $CaCO_3$ and Fe oxides and are referred to as FeCaCO. These samples with different x values, as well as the solid residues obtained after the reaction, were examined by X-ray diffraction using a Bruker D8 instrument. Mössbauer spectra were recorded in the transmission mode using a ^{57}Co γ-ray source in a rhodium matrix. The velocity and isomer shift were calibrated using iron foil. The Mössbauer spectra were analyzed using SITE and DIST options in the Win Normos-for-Igor software package. The carbonate content of the samples was estimated using a Thermo Scientific Flash 2000 CHNS analyzer, using an SQS column at 350 K and a thermal conductivity detector. The carbonates were decomposed to CO_2 at 1100 K in He gas. The gas samples were analyzed using a gas chromatograph manufactured by Mayura Analyticals Ltd (India). The products were separated using a Hayesep packed column using N_2 as the carrier gas. The column was connected to a Ru loaded methanator at 623 K and a flame ionization detector. The specific surface area was measured by the BET method by adsorbing N_2 at 77 K using Quantachrome autosorb IQ. The Fe/Ca ratio on the surface of the samples were obtained by recording the X-ray photoelectron spectroscopy (XPS) spectra using a EAC2000 SPHERA 547 spectrometer made by Omicron Nanotechnology ESCA, using Mg-Kα X-ray radiation at 300 K under a 10^{-10} mbar pressure. The area under the curve for the Fe2p and Ca2p spectra was calculated after baseline and sensitivity corrections. TEM images were recorded at 200 kV using a Technai instrument.

Catalytic reaction

In a typical experiment, 0.04 g of Fe containing $CaCO_3$ (FeCaCO) was heated in a continuous flow, packed bed, stainless steel reactor at a temperature ranging between 573 and 873 K in H_2 gas flowing at a rate of 3 mL min^{-1}. Unlike the earlier work, the reaction was carried out at atmospheric pressure. The gaseous decomposition products of the carbonates were collected in a gas bladder and were injected into the gas chromatograph after an interval of 1 h. The reaction was carried out for 2 h, after which the further decomposition of carbonates was not observed. No external reactant feed containing CO or CO_2 was used during the reaction. The conversion of carbonates to products such as CO, CO_2 and hydrocarbons was calculated by subtracting the amount of undecomposed carbonates remained after reaction from the total amount of carbonates. For convenience, the solid product remaining after the heat treatment in a H_2 atmosphere will be referred to as FeCaD.

Results and discussion

We have carried out the hydrogen reduction of the FeCaCO samples prepared by co-precipitation, wherein the carbonate was in an intimate mixture with iron oxide. The carbonate itself contained Fe in the form of $Ca_{1-y}Fe_yCO_3$.[21] The proportion of Fe in FeCaCO was varied over a wide range of Fe/Ca mole ratios (x = 0.0–5.0). The starting carbonate was found to possess the calcite structure, as expected,[20] and excess Fe was present as Fe_2O_3. When x was small ($x < 2$), the calcite phase was the major component while the Fe_2O_3 component increased with x. The X-ray diffraction data was also supported by the Mössbauer data. The specific surface area of xFeCaCO was found to be 95 m^2 g^{-1} for x = 5 and 13 m^2 g^{-1} for x = 0.5. The pores were in the range of 5–10 nm.

The temperature of the reaction was chosen to be 673 K, as the conversion and yield were highest at this temperature (Table S1, ESI†). In Fig. 1, we show the total mole conversion of carbonate (CO_3) to gaseous products for different values of x, when the FeCaCO compositions were heated in H_2 at 673 K for 2 h. The gaseous products that were detected include CO_2, CO, CH_4, C_2H_4,

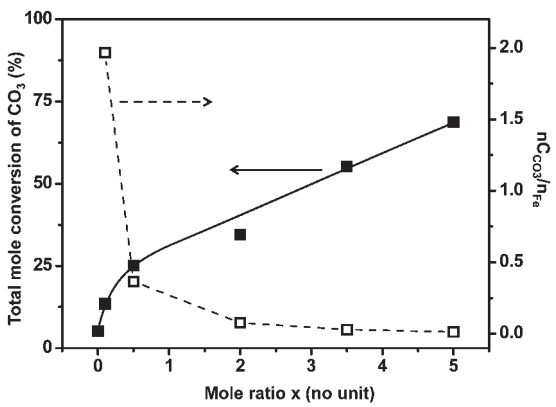

Fig. 1 Variation of the total mole conversion of CO_3^{2-} to products (CO, CO_2 and HCs) with x, at 673 K (■). The ratio of the number of moles of CO_3^{2-} in the sample to the number of moles of Fe (nC_{CO_3}/n_{Fe}) (□) is shown as a function of x.

Published on 12 March 2013. Downloaded by University of Western Ontario on 30/10/2014 19:55:39.

C_2H_6 and C_3H_8. The total mole conversion of CO_3 (%) was calculated as follows:

$$\text{Total mole conversion of } CO_3(\%) = \left(\frac{nC_{CO_3} - nC_{UD}}{nC_{CO_3}}\right) \times 100$$

Here, nC_{CO_3} is the total number of moles of carbon present in FeCaCO before the reaction and nC_{UD} is the total number of moles of carbon present in the sample after the reaction. The value of nC_{UD} was calculated by decomposing FeCaD at a higher temperature (900 K). The decomposition of CO_3 did not go to completion under the reaction conditions possibly because of the inhomogeneous distribution of catalytically active Fe across the CO_3 matrix, and nC_{UD} decreases as x increases. The total mole conversion of CO_3 represents the percentage of the moles of CO_3 in FeCaCO that decomposed under the reaction conditions to form various products. The total mole conversion of CO_3 for FeCaCO is around 5% when $x = 0.0$ (*i.e.* pure $CaCO_3$) and increases as x increases, suggesting that the presence of Fe favors the decomposition of CO_3. From elemental analysis, it was found that for the same weight of FeCaCO, the number of moles of CO_3 decreases as the value of x increases. As a result, the number of moles of Fe present for every mole of CO_3 (nC_{CO_3}/n_{Fe}) increases with x as shown in Fig. 1 (broken line) which explains the increase in the total mole conversion of CO_3 with x. The slope of the increase in the mole conversion is large for smaller values of x, which suggests a higher activity for Fe.

Treatment of the starting carbonate material FeCaCO with hydrogen was found to yield CO and CO_2 as well as hydrocarbons. In Fig. 2, the specific mole conversion of CO_3 (%) is plotted against the mole ratio x. The specific mole conversion of CO_3 (%) is calculated as follows.

$$\text{Specific mole conversion of } CO_3 \text{ to HC}(\%) = \left(\frac{nC_{CO_3} - (nC_{UD} + nC_{CO} + nC_{CO_2})}{nC_{CO_3}}\right) \times 100$$

Here, nC_{CO} and nC_{CO_2} represent the total number of moles of CO and CO_2 respectively.

Table 1 Gaseous products formed for different values of x at 673 K in 2 h[a]

x	Yield (%)					
	CH_4	C_2H_4	C_2H_6	C_3H_8	CO	CO_2
0	0	0	0	0	0	5
0.1	1	2	2	0	1	7
0.5	2	3	5	0	2	12
2	2	3	2	1	8	17
3.5	4	5	3	1	7	34
5	5	7	4	4	6	21

[a] Yield was obtained by multiplying the total mole conversion of CO_3 and the selectivity for the products.

In a trend similar to the total mole conversion of CO_3, the specific mole conversion of CO_3 to HCs also increases with x, as shown in Fig. 2. In the absence of Fe ($x = 0.0$), the specific molar conversion to HC is zero. At $x = 0.0$, CO_2 is the main product formed, with only traces of CO. The presence of Fe is clearly essential for the conversion of CO_3 to CO and HCs. In other words, Fe is not only essential for enhancing the decomposition of CO_3 to CO_2, but also for the subsequent hydrogenation to yield the HCs. Increasing x or the concentration of Fe in FeCaCO does not result in a linear increase in the conversion to HCs. In order to estimate the catalytic activity of Fe, the specific mole conversion to HCs was normalized with respect to n_{Fe} in the sample. In Fig. 2, the turnover number for HCs (HC TON) is plotted against x (broken line). The plot represents the number of moles of carbon in CO_3 converted to HCs by one mole of Fe (present in FeCaCO) per second. The HC TON is high when $x = 0.1$, and then decreases gradually and proceeds asymptotically as x increases. Although the specific mole conversion of CO_3 to HCs is higher at high Fe concentrations, the activity of Fe (conversion per n_{Fe}) does not follow the trend. This observation is consistent with our inference, based on the total mole conversion of CO_3 in Fig. 1, that the activity of Fe is high in the lower x regime.

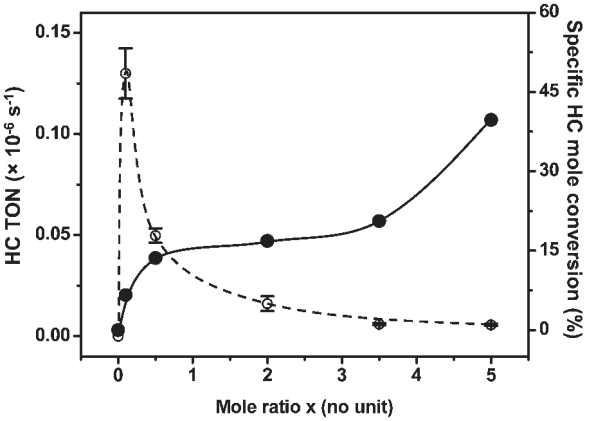

Fig. 2 Plot of turnover number of the HCs (HC TON) on the Fe catalysts (○) and the specific mole conversion of CO_3^{2-} to HC (●) against different mole ratios x, at 673 K.

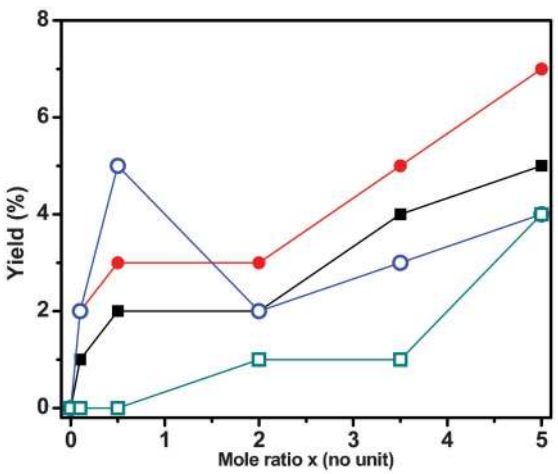

Fig. 3 Variation of the yields (%) of different HCs such as CH_4 (■), C_2H_4 (●), C_2H_6 (○) and C_3H_8 (□) with x, at 673 K.

This journal is © The Royal Society of Chemistry 2013

Published on 12 March 2013. Downloaded by University of Western Ontario on 30/10/2014 19:55:39.

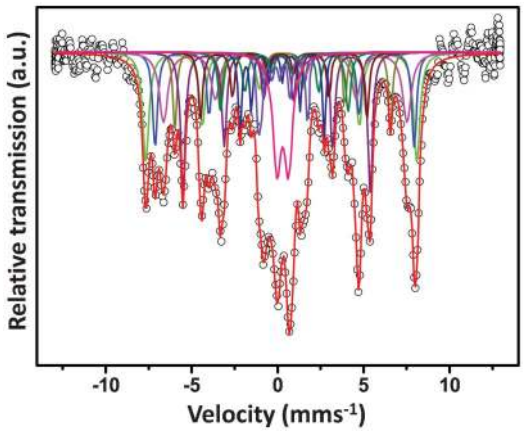

Fig. 4 Mössbauer spectra of FeCaD (x = 5) showing the various phases of iron. The black open circles show the observed data and the red solid line is the fit to the observed data. Each of the sub-spectra from left to right are identified as γ-Fe_2O_3 (489 kOe), Fe_3O_4 (A-site)–γ-Fe_2O_3 (467 kOe), Fe_3O_4 (B-site) (437 kOe), α-FeOOH (390 kOe), α-Fe (335 kOe), θ-Fe_3C (302 kOe), θ-Fe_3C (230 kOe), χ-Fe_5C_2 (152 kOe), χ-Fe_5C_2 (90 kOe) and superparamagnetic Fe^{3+} (narrow doublet), respectively. The numbers in the brackets represent the corresponding hyperfine field values.

The yields of various products formed during the reaction are presented in Table 1. The yields of HCs are shown graphically in Fig. 3. The total yield of HCs increases as the value of x increases, suggesting a higher selectivity for HCs. Comparing the trends across the HCs, the relative yield of C_2H_4 was higher than the other HCs for all values of x, while the yield of C_3H_8 increased with x. This trend suggests that higher concentration of Fe favors C–C coupling over dehydrogenation. HCs higher than C_3H_8 were not detected. It is noteworthy that the total yield of HCs obtained here is comparable to that in the FT synthesis.

After 2 h of heat treatment, the decomposition products, FeCaD, were examined by X-ray diffraction and Mössbauer spectroscopy. The X-ray diffraction pattern of FeCaD (x = 0.5) showed the presence of Fe_3O_4 which may have formed by the reduction of Fe_2O_3. The X-ray diffraction pattern of FeCaD (x = 5.0) showed the presence of α-FeOOH, γ-Fe_2O_3, Fe_3O_4, α-Fe, θ-Fe_3C, χ-Fe_5C_2 and $CaFe_2O_4$. The presence of these phases was also supported by the analysis of the Mössbauer spectrum in Fig. 4 (See Tables S2 and S3, ESI†).

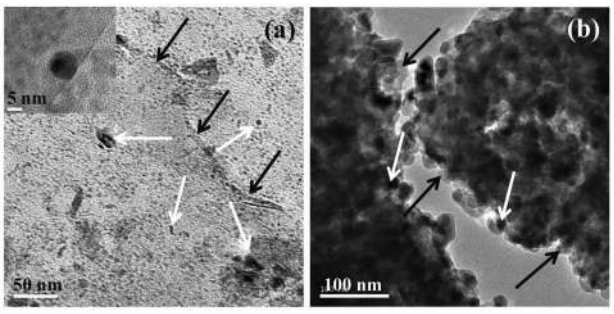

Fig. 5 TEM images of FeCaD showing the regions of dark contrast (white arrow) and the regions of lighter contrast (black arrow) for (a) x = 0.5 and (b) x = 5.

In Fig. 5, we present TEM images of two FeCaD samples (x = 0.5 and 5.0). The TEM images of both of the samples showed regions of darker contrast (white arrow marks) and regions of lighter contrast (black arrow marks). The darker regions may be Fe-rich regions because of the higher bulk density of the Fe phases observed in this reaction. The electron diffraction patterns and the elemental ratio of the samples at the different regions are presented in Fig. S4, ESI.† The size of these dark spots was 2–10 nm in diameter for x = 0.5 (Fig. 5a) and 30–50 nm for x = 5 (Fig. 5b). In contrast to the x = 0.5 sample, the regions of darker contrast are more densely crowded in the x = 5 sample. The change in the size of the Fe-rich particles with x explains the trend observed in the total mole conversion of CO_3 and the specific mole conversion of CO_3 to HCs (see Fig. 1 and 2), where an apparent decrease in the activity of the Fe catalysts (conversion per n_{Fe}) is observed with an increase in x. XPS spectra were recorded for the FeCaCO and FeCaD samples (x = 1 and 5) in order to determine the Fe/Ca ratio on the surface of the carbonates as the reaction proceeded (Fig. S5, ESI†). The Fe/Ca ratio is comparable for both the x = 1 and 5 FeCaD samples. The surface content of Fe varies as the reaction proceeds, an aspect which requires further investigation.

The decomposition of $CaCO_3$ containing transition metal ions occurs at a lower temperature in a H_2 atmosphere.[22,23] During the reaction, the carbonate decomposes to CO_2, which undergoes reduction to form CO and HCs. The formation of CO is crucial for the formation of the HCs as CO and H_2 which adsorb on the surface of the catalyst can give rise to RCH_2 species (R = H, CH_2 or CH_3).[24] The chain growth, followed by their desorption from the surface of the catalyst, results in HCs of varying molecular weights. A dynamic equilibrium between CO_2 and CO involving H_2 and $H_2O_{(g)}$ is possible under the reaction conditions in the form of the water–gas shift reaction.[25] In a separate experiment, when we passed a mixture of CO and $H_2O_{(g)}$ over FeCaD (x = 2) at 673 K, CO was converted to CO_2. Similarly, formation of CO was observed when a mixture of CO_2 and H_2 was passed over the catalyst under the same conditions. This observation is to be expected as Fe-based catalysts in FT reactions are known to catalyze the water–gas shift reaction.[25] Interestingly, trace amounts of HCs were also observed at 673 K within 15 min of reaction. The equilibrium between CO_2 and CO plays an important role in adjusting the CO/H_2 ratio, which in turn affects the formation of HCs. Under the present experimental conditions, excess H_2 and the low temperature (673 K) may not favour the reverse water–gas shift reaction.[26] The theoretical conversion of the reverse water–gas shift reaction calculated at this temperature is less than 5%.[27]

In the present study, the decomposition of CO_3 to CO_2 started at around 400 K, and the formation of CO occurred at around 500 K for all values of x. In Fig. S7, ESI,† we compare the temperature-dependent product formation during the decomposition of $CaCO_3$ and xFeCaCO (x = 5). For x = 0.0, CO_2 was the only product observed (see Fig. 1), suggesting that Fe was necessary for the hydrogenation of CO_2 to CO. Note that the reduction of Fe ions in FeCaCO to form different phases of iron occurs simultaneously with the decomposition of CO_3. The final products based on Fe could be affected by the concentration of H_2, CO_2 and CO.[28] As the

Published on 12 March 2013. Downloaded by University of Western Ontario on 30/10/2014 19:55:39.

concentration of CO_2 and CO changes during the reaction, it is difficult to control the composition of the active catalyst. Since the proportion of the active metal phase formed increases with x (as evidenced by the formation of Fe_3O_4, Fe and Fe_5C_2), the specific mole conversion of CO_3 to HCs also increases with x. Fe_2O_3 and Fe_3O_4 formed in the reaction can actively reduce CO_2 to CO, as Fe_3O_4 is an active water–gas shift catalyst.[25] The formation of CH_4 and other higher HCs was observed above 500 K, around which temperature the reduction of oxides to metallic Fe occurs (523–623 K).[20] Metallic α-Fe can therefore be actively involved in the formation of CH_4 and HCs. Thus, the mixtures of Fe metal and iron oxides supported on Ca-rich oxides catalyze the conversion of CO_2 to CO and HCs. We observe the presence of crystalline $CaFe_2O_4$ at higher concentrations of Fe.

Since the amounts of CO_2 and CO produced increases with x, and the proportion of CO_2 is always significantly greater than that of CO and the HCs for a particular value of x, it is likely that the rate of decomposition of CO_3 to CO_2 is generally higher than that of the reduction of CO_2 to CO or HCs. This explains the high yield of CO_2 (Table 1). The results of the HC yields presented in Table 1 can be explained based on the value of x and the types of phases that are formed.[29] From Fig. S2 and S3, ESI,† it can be observed that there is an increase in the tendency for the formation of carbide phases of Fe as x increases. Since Fe_5C_2 is associated with C–C coupling, we speculate that the particle size plays an important role in the selectivity of the reaction.[20,30] θ-Fe_3C can however result from the deactivation of χ-Fe_5C_2.[31] We do not observe the carbide phases at low values of x ($\sim$0.5). The lower chemisorption potential of H_2 on the smaller-sized catalysts favors the reduction of the oxides of carbon, compared to the larger-sized particles.[32] From this result, one should expect higher HC yields at low x values. However, from Table 1, we observe that the HC yield is higher as x is increased. The observation in our work differs from the earlier work because an increase in the concentration of Fe also increases the rate of decomposition of CO_3, as observed from the nC_{UD} values. The formation of C_2H_4 is explained on the basis of the rearrangement or β-elimination of C_2 intermediates adsorbed on the iron.[33] A higher selectivity for C_2H_4 at low values of x found in this study are in accordance with the results on the size dependent selectivity of Fe-based FT catalysts.[29] Smaller particles have a lower H_2 chemisorption potential which favors the formation of olefins, rather than C–C coupling.[32] Although the results present only the trends on the product formation, we shall attempt to explain the selectivity of the process in relation to particle size and chemisorption. The explanation is based on the general conclusions drawn by earlier workers. The formation of C_2H_6 and C_3H_8 is probably preceded by the formation of C_2H_4. Hydrogenation of C_2H_4 to yield C_2H_6, or chain elongation to higher hydrocarbons, is favored depending on the chemisorption of H_2 and CO, which in turn is a function of particle size and crystalline phase of the catalyst. The chemisorption potentials of H_2 and CO are closely related as the M–CO bond is electron-accepting while the M–H bond is electron-donating.[32] Thus, as the value of x increases, both C_2H_6 and C_3H_8 are formed in relatively higher yields. It is noteworthy that the decomposition of CO_3 to HCs is highly selective for the formation of C_1–C_3 HCs, which are important starting materials in the chemical industry. Possible reasons for this selectivity could be the following: (a) a H_2-rich atmosphere is conducive for the hydrocracking of longer HCs, and (b) reaction mixtures which are rich in H_2 do not attain the necessary CO : H_2 ratios to form longer HCs.

Although lower hydrocarbons have uses as feed stock chemicals in industry, it is useful to calculate the energy obtained during their combustion to calculate the energy efficiency of the process. The energy balance (E_b) of the reaction can be defined as the energy gain or loss that occurs in synthesizing (E_p) and hydrogenating (E_h) one mole of $CaCO_3$ and the energy obtained during the combustion (E_c) of the hydrocarbons produced in the reaction.

$$E_b = E_p + E_h - E_c$$

The reaction involving the synthesis of $CaCO_3$ from the precursors can be represented by the following equation.

$$10NaHCO_3 + 2Ca(NO_3)_2 + 3FeCl_2 \rightarrow 3FeCO_3 + CaCO_3 + 4NaNO_3 + 4NaCl + 5H_2O + Na_2CO_3 + 5CO_2 + CaCl_2$$

$$E_p = 142 \text{ kJ mol}^{-1}$$

Assuming 100% hydrogenation, and the same ratio of products as obtained in the experiments for FeCaD with x = 5, the hydrogenation of $CaCO_3$ may be represented by the following equation.

$$CaCO_3 + 2H_2 \rightarrow CaO + 0.29CO_2 + 0.12CO + 0.06CH_4 + 0.12C_2H_4 + 0.06C_2H_6 + 0.06C_3H_8 + 1.3H_2O$$

$$E_h = +72 \text{ kJ mol}^{-1}$$

It can be found that an energy, E_c = 449 kJ, can be obtained during the combustion of 0.06 moles of CH_4, C_2H_6 and C_3H_8 and 0.12 moles of C_2H_4. Thus, an energy, E_b = 231 kJ, can be gained by producing and utilizing one mole of $CaCO_3$. Furthermore, CO_2 produced during the combustion of the hydrocarbons can be directly used to produce hydrocarbons, or used in the carbonation of CaO. We note that the energy efficiency of the process can be further improved if the selectivity is shifted towards higher hydrocarbons. The calculation, however, does not take into account the energy that may be consumed in the production of H_2 (which can be reduced with new emerging technologies regarding the production of H_2) or the extraction of mineral carbonates, which is beyond the scope of the present work.

Conclusions

From the present study, we conclude that Fe-containing $CaCO_3$ is a useful material for the conversion of CO_3 to HCs with selectivity for C_1–C_3 products. Such carbonate materials can be prepared readily even if they do not exist in nature. Iron, present in the form of metal, metal oxides and metal carbide particles supported on Ca-rich oxides, is involved in the decomposition of CO_3 to CO_2 and

 This journal is © The Royal Society of Chemistry 2013

Published on 12 March 2013. Downloaded by University of Western Ontario on 30/10/2014 19:55:39.

its subsequent reduction to CO and HCs. Since many of the iron-based phases are present in active Fischer–Tropsch catalysts, it is possible that the conversion of CO_3 to HCs follows a similar mechanism. However, more detailed studies are required to establish the mechanism of the processes described here. The process reported by us will be economically attractive and environmentally benign if the selectivity for higher hydrocarbons is improved. We are carrying out research along this pathway. By suitably controlling the decomposition of carbonates and the formation of iron-based catalytic phases, it may be possible to achieve better selectivity and higher levels of conversion.

Acknowledgements

DJ thanks Mr. V. Shinde (IISc) and Mr. P. Chaturbedy (JNCASR) for useful discussions, Mr. Ritesh (JNCASR) and Mr. B. V. S. S. P. Kumar (JNCASR) for surface area measurements, Mrs U. Tumurkar and Dr. J. Ghatak (JNCASR) for TEM measurements and Mr. G. Kishore Kumar (JNCASR) for XPS measurements.

Notes and references

1 M. Aresta and A. Dibenedetto, *Dalton Trans.*, 2007, 2975.
2 T. Sakakura, J.-C. Choi and H. Yasuda, *Chem. Rev.*, 2007, **107**, 2365.
3 D. J. Darensbourg, *Chem. Rev.*, 2007, **107**, 2388.
4 D. T. Whipple and P. J. A. Kenis, *J. Phys. Chem. Lett.*, 2010, **1**, 3451.
5 A. J. Hunt, E. H. K. Sin, R. Marriott and J. H. K. Clark, *ChemSusChem*, 2010, **3**, 306.
6 C. D. N. Gomes, O. Jacquet, C. Villiers, P. Thuéry, M. Ephritikhine and T. Cantat, *Angew. Chem., Int. Ed.*, 2012, **51**, 187.
7 A. B. Rao and E. S. Rubin, *Ind. Eng. Chem. Res.*, 2006, **45**, 2421.
8 G. T. Rochelle, *Science*, 2009, **325**, 1652.
9 J. Čejka, A. Corma and S. Zones, *Zeolites and Catalysis: Synthesis, Reactions and Applications*, Wiley-VCH, Weinheim, Germany, 2010.
10 K. Sumida, D. L. Rogow, J. A. Mason, T. M. McDonald, E. D. Bloch, Z. R. Herm, T.-H. Bae and J. R. Long, *Chem. Rev.*, 2012, **112**, 724.
11 K. Raidongia, D. Jagadeesan, M. U-Kahalay, U. V. Waghmare, S. K. Pati, M. Eswaramoorthy and C. N. R. Rao, *J. Mater. Chem.*, 2008, **18**, 83.
12 A. Ghosh, K. S. Subrahmanyam, K. Saikrishna, S. Datta, A. Govindaraj, S. K. Pati and C. N. R. Rao, *J. Phys. Chem. C*, 2008, **112**, 15704.
13 J. I. Park, D. Jagadeesan, R. Williams, W. Oakden, S. Chung, G. Stanisz and E. Kumacheva, *ACS Nano*, 2010, **4**, 6579.
14 G. Aydin, I. Karakurt and K. Aydiner, *Energy Policy*, 2010, **38**, 5072.
15 R. Zevenhoven, S. Eloneva and S. Teir, *Catal. Today*, 2006, **115**, 73.
16 D. Jagadeesan, M. Eswaramoorthy and C. N. R. Rao, *ChemSusChem*, 2009, **2**, 878.
17 (*a*) F. Fischer, *The Conversion of Coal into Oils*, (translated by R. Lessing), Ernest Benn Ltd., London, 1925; (*b*) F. Fischer and H. Tropsch, *Brennst.–Chem.*, 1926, **7**, 97.
18 (*a*) H. M. T. Galvis, J. H. Bitter, C. B. Khare, M. Ruitenbeek, A. I. Dugulan and K. P. de Jong, *Science*, 2012, **335**, 835; (*b*) H. Schulz, *Appl. Catal., A*, 1999, **186**, 3.
19 K. Fang, D. Li, M. Lin, M. Xiang, W. Wei and Y. Sun, *Catal. Today*, 2009, **147**, 133.
20 E. de Smit and B. M. Weckhuysen, *Chem. Soc. Rev.*, 2008, **37**, 2758.
21 K. Vidyasagar, J. Gopalakrishnan and C. N. R. Rao, *Inorg. Chem.*, 1984, **23**, 1206.
22 A. Reller, C. Padeste and P. Hug, *Nature*, 1987, **329**, 527.
23 C. Padeste, A. Reller and H. R. Oswald, *Mater. Res. Bull.*, 1990, **25**, 1299.
24 B. H. Davis, *Catal. Today*, 2009, **141**, 25.
25 V. R. R. Pendyala, G. Jacobs, J. C. Mohandas, M. Luo, W. Ma, M. K. Gnanamani and B. H. Davis, *Appl. Catal., A*, 2010, **389**, 131.
26 V. M. Shinde and G. Madras, *Appl. Catal., B*, 2012, **123–124**, 367.
27 C. Rhodes, G. J. Hutchings and A. M. Ward, *Catal. Today*, 1995, **23**, 43.
28 D. B. Bukur, K. Okabe, M. P. Rosynek, C. P. Li, D. J. Wang, K. Rao and G. P. Huffmann, *J. Catal.*, 1995, **155**, 353.
29 M. A. McDonald, D. A. Storm and M. Boudart, *J. Catal.*, 1986, **102**, 386.
30 C. K. Rofer-DePoorter, *Chem. Rev.*, 1981, **81**, 447.
31 H. Jung and W. J. Thomson, *J. Catal.*, 1992, **134**, 654.
32 M. E. Dry, T. Shingles and L. J. Boshoff, *J. Catal.*, 1972, **25**, 99.
33 H. Schulz and A. Z. El Deen, *Fuel Process. Technol.*, 1977, **1**, 45.